

# Chromatic techniques for in-vivo monitoring jaundice in neonate tissues

A T Sufian<sup>1</sup>, G R Jones<sup>1</sup>, H M Shabeer<sup>2</sup>, E Y Elzagzoug<sup>1</sup>, J W Spencer<sup>1</sup>

<sup>1</sup> Department of Electrical Engineering and Electronics, Centre for Intelligent Monitoring Systems, University of Liverpool, Liverpool L69 3GJ, UK

<sup>2</sup> Thegana Medical Mission Hospital & Research Centre, Perumpanachy. P.O, Changanacherry, Kottayam, Kerala, India.

E-mail: [a.sufian@liverpool.ac.uk](mailto:a.sufian@liverpool.ac.uk)

## Abstract

A chromatic method is described for providing a preliminary indication of unacceptable bilirubin levels in a newly born baby in order to avoid the development of serious mental deficiencies. The aim was to investigate the reliability of a new chromatic approach using a novel template unit for a preliminary, non-invasive monitoring of the skin tissue of newly born babies with jaundice and its capability for use with different mobile phone cameras. A description of the monitoring system is given along with an explanation of the monitoring technique used.

Preliminary tests have been performed on 48 different neonates each being addressed by one of 6 different mobile phone cameras, which were randomly available to the operating clinicians

The significance of the results obtained is that they show the approach to have a high level of fail-safe reliability in indicating the **bilirubin** levels when compared with **blood** test results. The test results have a **correlation (R<sup>2</sup>)** of 0.81, a **Sensitivity (Sn)** of 0.97, a **Specificity (Sp)** of 0.82, a Positive Predictive value (**PPV**) of 0.95 and a Negative Predictive Value (**NPV**) of 0.9. The results also show that the approach can be used with a few different mobile phone cameras and that because of its non-invasive nature and its cost effectiveness, has the potential for remote use from a medical hospital to provide an immediate preliminary diagnosis.

**Keywords:** chromatic techniques, new born jaundice, condition monitoring, mobile phones

## 1. Introduction

Although the occurrence of jaundice in newly born babies could lead to severe brain damage (Dennery et al 2001, Polley N et. al 2015) prolonged hospitalisation for **bilirubin** blood testing (Total Serum Bilirubin TSB) to check for unacceptable jaundice levels (typically > 10 mg/dl) for many babies is not necessary (Dennery et al, 2001). Because such blood testing is invasive it is painful and stressful for the neonate and can result in blood loss and increased risk of developing infections (Dai et al, 1997, Lilien et al 1976). A non-invasive, less laborious and time consuming means of providing an immediate, preliminary diagnosis is therefore desirable.

Possible alternatives to invasive blood sampling have been reported which are in vivo, non-invasive and optically addressing various tissue areas on the torso of newly born babies (**Transcutaneous Bilirubinometry (TcB)**). Such methods use various optical techniques to monitor the absorbance of various optical wavelengths for indicating the bilirubin concentration. Various approaches use different types of light sources (Xenon, Tungsten Halogen, Light Emitting Diodes (LEDs)) with various forms of optical spectroscopy to address different torso areas such as the eye conjunctiva, ear lobes, nose, forehead, and abdomen.

The first **transcutaneous bilirubin meter** was introduced in 1980 (Yamanouchi et al, 1980) and since then, several other devices have been developed (Yasuda et al 2013, Tayaba et al 1998, Rubaltelli et al 2001, De Luca et al 2008, Bertini et al 2008, Petersen et al 2015). Bosschart et al 2011 used a tungsten halogen source with an optical fiber probe and spectrograph. Polley et al 2015 used optical fibre probes and a spectrograph for measuring differences in light absorbance by the conjunctiva of the eye in the wavelength range 460 to 600nm for online monitoring of jaundice and a similar approach was used for hemoglobin estimation (Sarkar et al 2017). Pratesi et al (2015) have employed BiliCare™ system which uses green and blue light emitting diode (LED) sources to measure the ratio of light intensity before and after transmission through a neonate's ear lobe and compared it with a JM-103™ system which uses a **xenon** lamp and measures the green and blue light components reflected from a neonate's forehead. In addition a **xenon** lamp and LED have been used for addressing light reflected from the skin (Biliscan 2017), more recently a smartphone camera has been used for obtaining an image of a neonate's torso with ambient light (de Greef et al 2014, Taylor et al. 2017) from which the colour of the skin was determined and related to the bilirubin level..

Such devices could reduce the number of hospital readmissions (Petersen et al 2005) and decrease the amount of required blood samples from patients (Maisels and Kring 1997). Their use is recommended in clinical practice guide lines on the management of hyperbilirubinemia (Maisels et al 2004). However, no transcutaneous bilirubin meter has yet evolved with sufficient reliability for reducing the usage of invasive blood sampling through a preliminary assessment of **bilirubin** level in vivo. Performance improvements of **TcB** methods remain to be sought (de Greef et al 2014, Bosschaart et al 2012) particularly with regard to indicating the need for detailed blood testing.

The present contribution addresses this need for a more reliable approach for the preliminary optical monitoring of skin tissue bilirubin. The approach is based upon a non-linear form of **chromatic** analysis (Deakin et al 2014, Jones et al 2009a, Elzagzoug et al 2014, Lo et al 2017) which derives from initial chromatic investigations at the Royal Liverpool Women's Hospital in 1998 (Jones et al 2008). It uses a light tight housing containing LEDs for illumination and an optical reference template onto which a mobile phone camera can be attached. The template assists in automatically tuning the mobile phone camera plus providing measurement references. The unit carries a transparent plastic window through which an occluded tissue area (e.g. nose, forehead, abdomen) is addressed. The approach can be used with different types of mobile phone cameras, has good reliability and has a potential for use remote from medical hospitals.

Preliminary results for **bilirubin** levels obtained with this system for 48 neonates and 6 different types of mobile phone cameras are presented and compared with the Bilirubin levels determined from blood tests.

## **2. Experimental Methods**

### *2.1 Optical Measurement Technique*

The optical measurement technique used in the present study was based upon chromatically monitoring white light from a group of Light Emitting Diodes (LEDs) reflected /scattered from the skin tissue of a neonate in vivo using a mobile phone camera. A schematic diagram of the in vivo tissue monitoring system is shown in figure 1(a).

The system consisted of a removable mobile phone camera mounted upon a light tight housing for monitoring a reference template carrying a rigid plastic window at the other end of the light tight enclosure. The rigid plastic window was pressed against the tissue under test (e.g. neonate nose) in order to occlude haemoglobin from the tissue and so enhance the optical influence of the tissue. The template, including the plastic window was illuminated by an array of white light surface mount diodes arranged in a strip (0.2W, from Sunlux Energy Ltd) and circled around an aperture (figure 1 (a)) through which the camera lens observed and captured an image of the template and window.

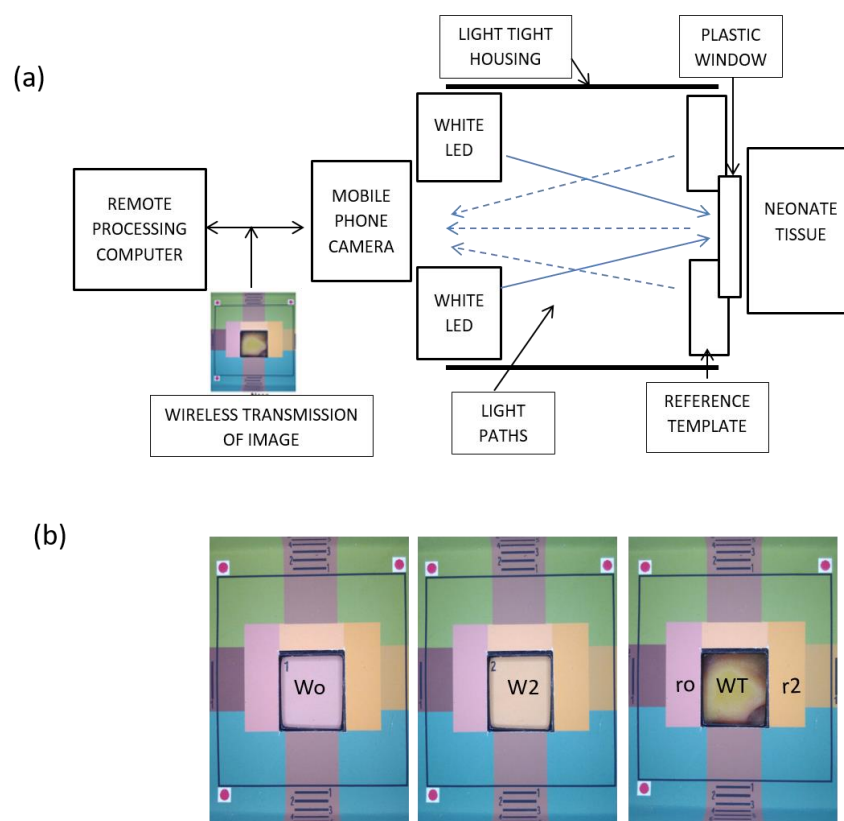


**Figure 1.** Optical measurement system and image produced

(a) Schematic diagram of the system layout

(b) Typical images captured by a mobile phone camera of  $W_0$  (set  $B_I = 0$ ),  $W_2$  (set  $B_I = 10\text{mg/dl}$ ) and  $WT$  (neonate nose tissue) in the sample window and set references  $r_0 = (\text{set } B_I \approx 0)$ ,  $r_2 = (\text{set } B_I \approx 10)$

The template consisted of a colour printed-paper with a rectangular and rigid sample viewing plastic window (figure 1 (b)). The printed paper had several sectors with different chromatic signatures, which were empirically chosen, along with some alignment assisting features. Two template sectors adjacent to the plastic window had chromatic signatures chosen empirically from occluded skin images of two neonates one without jaundice ( $r_0$ ) and one with 10mg/dl bilirubin ( $r_2$ ). These areas provided an indication relative to a sample in the window as to whether the camera settings etc. had varied so that compensation could be made. The remaining template areas were empirically coded to accommodate

automatic image adjustments made by the camera operating system and which could vary for different cameras.

The 6 mobile phone cameras used in the tests are listed on Table 1 A, Appendix 1 along with the pixel density and the number of different neonates tissues addressed by each camera. Each mobile phone camera was operated in “auto mode” so that the exposure time was automatically set. Geometric alignment features on the template (figure 1 (b)) (red dots, square black frame) enabled the camera to be checked for correctly addressing relevant areas on the template sectors (ro, r2, W figure 1 (b)) for chromatic analysis.

Relevant areas of sectors on the image captured by the mobile phone camera (sample window (WT), reference sectors (ro, r2) figure 1(b)) produced outputs for three parameters (R, G, B) whose wavelength responses were non-orthogonal as shown on figure 2 and covered the wavelength ranges of various skin tissue components (bilirubin, hemoglobin, melanin (Bhutani et al 2000)). The R, G, B outputs were processed to yield chromatic parameters X, Y, Z and L to quantify the variation between different images. X, Y, Z and L are defined by (Jones et al 2008).

$$L = (R + G + B)/3 \quad (1)$$

$$X = R/3L; \quad Y = G/3L; \quad Z = B/3L \quad (2)$$

This enabled features of complicated spectra to be defined and quantified in terms of a limited number of parameters whilst remaining sensitive to the growth of unexpected spectral features and events. Sensor responses and chromatic parameters may be selected for highlighting the required information (Deakin et al 2014, Jones et al 2009a, Elzagzoug et al 2014, Lo et al 2017). The chromatic parameters X, Y, Z may be represented on a two dimensional chromatic map, for example a graph of Y against Z which emphasises variations at short / medium wavelengths (B, G) with respect to the overall wavelengths (B, G, R). The bilirubin spectrum is mainly covered by the B and G detectors, while the hemoglobin and melanin spectra extend across the B, G and R detectors (figure 2).

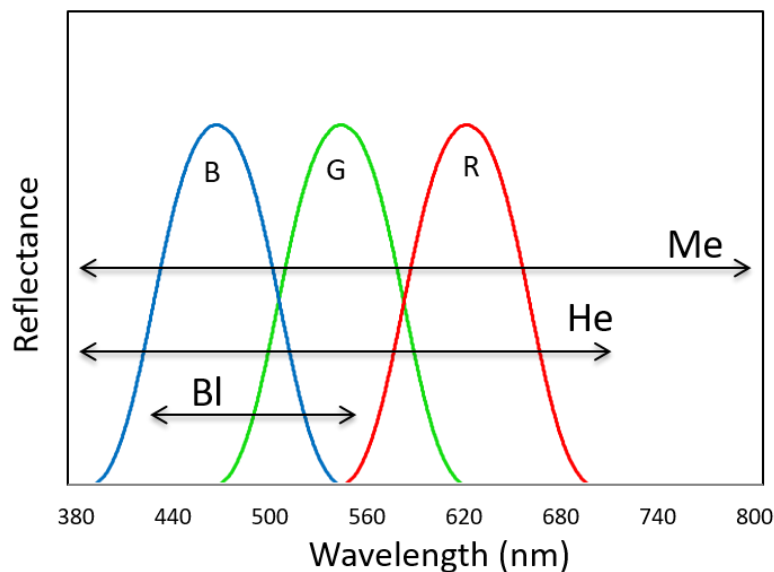


**Figure 2.** Typical overlapping wavelength responses (R, G, B) of an electronic camera relative to wavelength ranges of some skin tissue components (Bilirubin (Bl), Hemoglobin (He), Melanin (Me)).

The image captured by the mobile phone camera could be transmitted to a remote central hub computer for chromatic processing and derivation, via calibration, of the **bilirubin** level (indicative of jaundice) in the tissue. The result was automatically transmitted back to the sender within a couple of seconds so enabling the mobile phone system to be utilised at rural regions remote from a medical hub.

The setting up procedure for using the camera system involved automatically checking for image acceptability with regard to the reference sectors ( $r_0$ ,  $r_2$ ) (figure 1 (b)) and with paper reference samples of “normal” neonate skin  $W_0$  ( $B_I \sim 0$  mg/dl) and skin with moderate **bilirubin** level  $W_2$  ( $B_I \sim 10$ mg/dl) sequentially in the sample window. When introducing a new camera etc. three images were captured corresponding to three different samples in the template window, namely paper representations of  $W_0$  and  $W_2$  plus a real skin tissue  $W_T$  (figure 1 (b)). The R, G, B values for a specified area on each of the sectors ( $r_0$ ,  $r_2$ ,  $W$ ) were automatically extracted, stored and used to calculate the chromatic parameters X, Y, Z for further analysis by the computer software.

### *2.2. Test Procedures*

Tests were conducted on 48 newly born babies by clinicians at the Ovum Hospital, Bangalore, India and coordinated via the Thengana Medical Mission Hospital and Research Centre, Karala (TMMHRC). The subjects were drawn from infants born at the Ovum Hospital, Bangalore, who weighed at least 2500 g at birth, with a gestational age of at least 36 weeks. The cases were infants with a maximum TSB level of 16 mg/dl in the first 3 days after birth. Infants were excluded if they were receiving phototherapy.

Tests were conducted in accordance with ethical principles in the Declaration of Helsinki. Ethical approval was given via the Independent Ethics Committee Consultants (IECC) organised and operated according to the requirements of ICH – GCP, Indian Council of Medical Research. After the physician ordered a Total Serum Bilirubin (TSB) for clinical purposes, informed consent was obtained from a parent. The objectives and detailed procedures were explained to each parent in simple language and a copy provided to the parent entering the study which was signed by the parent.

For the optical camera tests, the tissue at the nose, forehead and abdomen of each neonate was occluded by pressing the stiff plastic sample window of the monitoring template against the neonate skin.

Following a camera test, blood samples were collected from neonates by veni puncture and were sent to the clinical laboratory at site for analysis. Serum was separated from blood and mixed with standard diazo reagent to form coloured compound (Puppalwar et al. 2012, Watson 1961). TSB levels were then measured with an abachem 200 semi-automated biochemistry analyser (abaxis healthcare ltd, India).

### *2.3. Operation of the Monitoring Unit*

Details of the deployment of the mobile camera and template unit for the in vivo testing of a tissue sample was as follows –

- a) A mobile phone camera was positioned on top of the template unit (figure 1(a)) and the geometric alignment of the frame and orientation was checked visually on the camera screen and adjusted by zoom camera control in order to capture the template image (figure 1(b)). Acceptable Images were automatically determined with the operating software.
- b) When testing with a new mobile phone camera, the unit was first used to address two calibration samples in the sample window. These were paper printed versions of 0 and 10 mg/dl **bilirubin**

levels ( $W_0$ ,  $W_2$  (figure 1 (b)) chromatically identical to reference areas  $r_0$ ,  $r_2$  (but with optical transmission through the plastic window).

- c) Images of  $W_0$  and  $W_2$  were captured by the camera from which R, G, B values of fixed areas on the window ( $W_0$ ,  $W_2$ ) and the reference ( $r_0$ ,  $r_2$ ) sectors were derived.  
Since the 6 different mobile phone cameras used in the tests had various pixel densities (Appendix 1, Table 1 A) the number of pixels ( $N_p$ ) addressed within the chosen monitored area from which the R, G, B values were calculated were determined using a fixed area ratio ( $A$ ), which varied with the pixel density ( $N_c$ ) of the particular type of camera (i.e.  $N_p = N_c / A$ ).  $N_p$  was automatically determined with the operating software.
- d) The skin tissue to be tested was occluded by pressing the plastic sample window onto the tissue and an image captured with the camera to obtain the R, G, B values of the sample ( $W_t$ ) and the corresponding two reference sectors ( $r_0$ ,  $r_2$ ).
- e) The R, G, B values for the camera calibration and tissue sample (sections (c) and (d) above) images were transmitted directly from the mobile phone to a hub computer which checked for correct operation, image alignment and calculated values of relevant chromatic parameters ( $Z$ ,  $Y$ ) from the R, G, B captured values (equations (1), (2)).
- f) The corrected chromatic parameters yielded **bilirubin** values by calibration with the 0 and 10mg/dl **bilirubin** paper samples values ((c). above).
- g) The calculated bilirubin value  $B_l$  was automatically transmitted back to the user via the mobile phone application, the entire process only taking a few seconds.
- h) The user was also automatically informed of any errors due to misalignment, unsuitable image etc.

Tests were performed on 48 different neonates by clinicians using mobile phone of their own choice. As a result the 6 different mobile phone cameras listed on Table 1 A, Appendix 1 were randomly used in the tests, the number of neonates monitored with each camera being indicated on the table.

### 3. Test Results and Data Analysis

The test results were analysed using two chromatic methods – Primary and Secondary Chromatic **analysis**. The Primary Chromatic **analysis** utilised the ratio of the medium wavelength parameter  $Y$  to the short wavelength parameter  $Z$  (cf. Pratesi et al 2015). The Secondary Chromatic Analysis utilised a more sophisticated correction procedure along with a non-linear calibration.

#### 3.1 Primary Chromatic Analysis

The Primary Chromatic **analysis** involved determining the medium and short wavelength chromatic parameters ( $Y$ ,  $Z$ ) from the R, G, B values of the window with a tissue sample ( $W_t$ ) (equations (1), (2) and Section 2.3).  $Y$ ,  $Z$  values were also obtained for images of set paper references  $W_0$  ( $B_l = 0$ ) and  $W_2$  ( $B_l = 10\text{mg/dl}$ ) in the window (figure 1 (b)) which were used to provide a linear calibration of ( $Y/Z$ ) versus **bilirubin** level. The Primary Chromatic bilirubin **level** (PCh $B_l$ ) is then given by.

$$PChBl = [(Y/Z)(WT) - (Y/Z)(Wo)]/[(Y/Z)(W2) - (Y/Z)(Wo)] \quad (3)$$

Where  $(Y/Z)(WT)$  = ratio of Y to Z with the tissue sample in the window (WT)

$(Y/Z)(Wo)$  = ratio of Y to Z with 0mg/dll Bl paper reference in the window (Wo)

$(Y/Z)(W2)$  = ratio of Y to Z with 10mg/dl paper reference in the window (W2)

Bilirubin values PChBl were obtained with equation (3) for the tests with 48 neonates each with one of the 6 different types of cameras (Table 1A, Appendix 1) as preferred by the clinician performing the test. The results are shown on figure 3 as a function of TSB levels obtained for each neonate from blood tests with the camera type used identified by the various symbols shown on Table 1A, Appendix 1. The skins were all occluded to reduce hemoglobin influence although melanin effects may have remained. This figure also shows, as dashed lines, the 95% Prediction Interval boundaries **PI(95%)** which define the scatter of the data from the fitted regression line (Altman 1991). The results show a high degree of scatter which may be due to several factors including the use of different types of cameras and possibly different melanin levels in individual neonates.

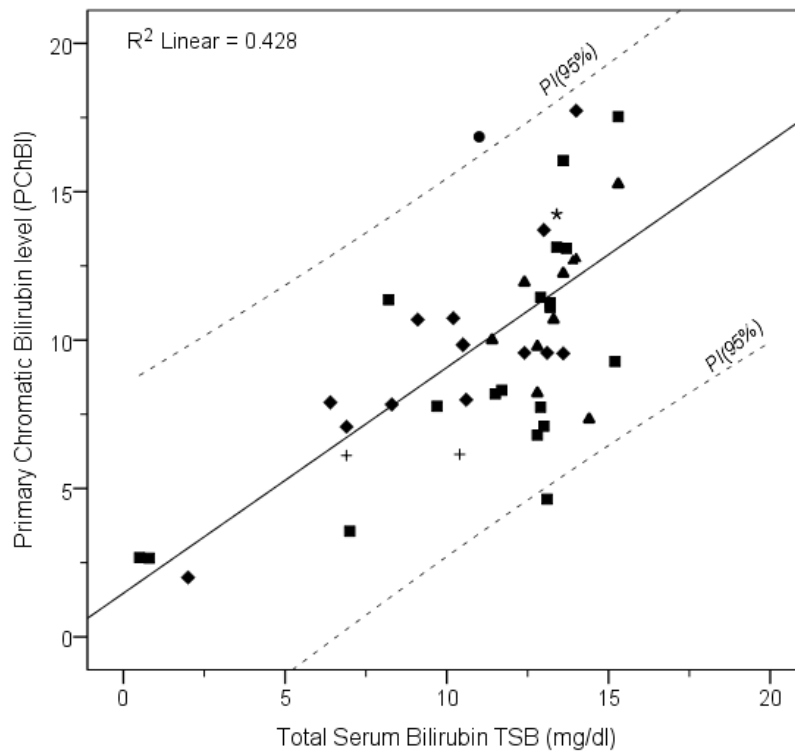


**Figure 3.** Primary Chromatic Bilirubin level (PChBl) versus Total Serum Bilirubin TSB(mg/dl). (Results for 48 neonate tests with 6 different phone cameras; each camera type designated by symbols from Table 1A). Solid line: Regression line, Dashed lines: Prediction Interval boundaries **PI(95%)**

### 3.2 Secondary Chromatic Analysis

The Secondary Chromatic **analysis** seeks to take account of additional complex factors which may adversely affect the accuracy of the **bilirubin** levels estimated from the camera images. For example, not only do various cameras have different pixel densities (Table 1A, Appendix 1) but they may also



have different relative numbers of R, G, and B pixels per unit area. The effect of such pixel variation, as well as other factors (e.g. window plastic quality, condition etc.), may be illustrated on a chromatic Y : Z map for the window addressed paper samples corresponding to 0 (Wo) and 10mg/dl (W2) bilirubin levels (figure 1 (b)). Figure 4 shows the Y : Z values derived with equations (1), (2) from the R, G, B values for Wo and W2 for each of the 6 mobile phone cameras used in the 48 neonates tests.

Also shown on figure 4 are the Y, Z window reference values Wo, W2 (figure 1 (b)) for an additional 6 mobile phone cameras listed on Table 1B, Appendix 1. These mobile phone cameras were not used in the neonate tests but are presented to show how the 6 tissue tests cameras are representative of a wider range of cameras. These results show the variability of the Wo – W2 loci obtained when using different mobile phone cameras compared with the locus of the set values of the paper references So – S2. The (So – S2) locus differs from the window loci (Wo – W2) due to the plastic window and other effects.

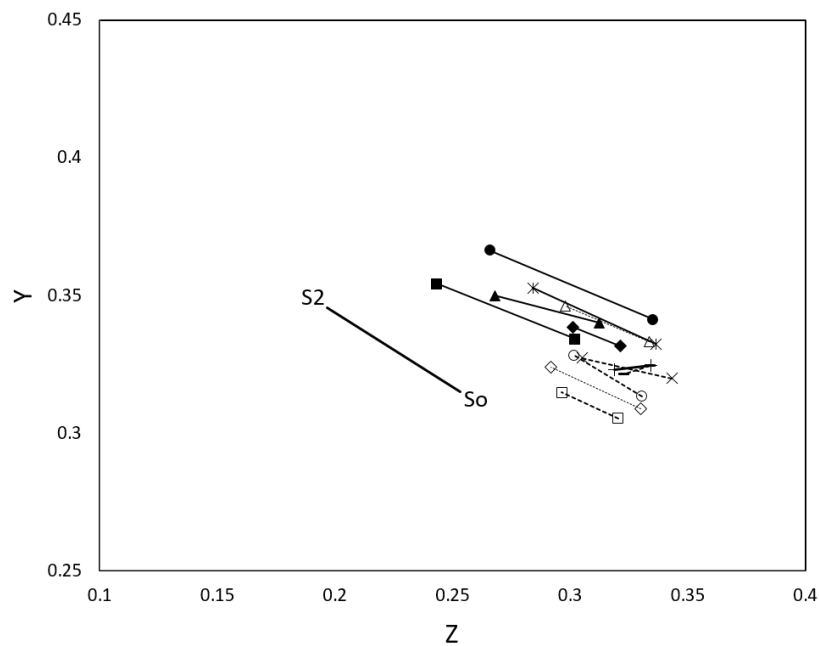


**Figure 4.** Chromatic Y : Z map showing set reference areas locus (So-S2) and set sample window loci (Wo-W2) for 12 different cameras with set reference (So-S2), 6 mobile phone cameras used in the neonate tests (Table 1A, Appendix 1) full lines, 6 mobile phone cameras used in reference tests only (Table 1B, Appendix 1) dashed lines.

The Secondary Chromatic analysis takes account of these various features. It involves two parts, namely the production of Correction Factors (CF) for the Z and Y chromatic parameters, and the calibration of the corrected Z and Y values to yield Secondary Chromatic Bilirubin levels (SChBl).

3.2.1. *Correction Factors (CF).* A procedure for correcting a test result obtained with a given camera, plastic window etc. to the set locus (So – S2) is illustrated on figures 5 (a), (b) and (c). These show chromatic maps based upon Y, Z parameters (equations (1), (2)) whose values were calculated from the R, G, B image values.

The procedure involved determining separate Correction Factors (CF(Z), CF(Y)) for the chromatic parameters Z and Y from the window paper references (Wo, W2) for a camera, relative to the set references (So, S2) (figure 5 (a)). The Correction Factors were defined as



$$\text{For } W_0 \text{ Z correction} \quad (CF(Z, W_0)) = (ZS_0)/(ZW_0) \quad (4.1)$$

$$\text{Y correction} \quad (CF(Y, W_0)) = (YS_0)/(YW_0) \quad (4.2)$$

$$\text{For } W_2 \text{ Z correction} \quad (CF(Z, W_2)) = (ZS_2)/(ZW_2) \quad (4.3)$$

$$\text{Y correction} \quad (CF(Y, W_2)) = (YS_2)/(YW_2) \quad (4.4)$$

The Z, Y coordinates of a tissue sample (WT) corrected with respect to S2 for example (figure 5 (b)) then become

$$\text{Z coordinate} \quad Z(WT^*2) = Z(WT) \cdot (CF(Z, W_2)) \quad (5.1)$$

$$\text{Y coordinate} \quad Y(WT^*2) = Y(WT) \cdot (CF(Y, W_2)) \quad (5.2)$$

In practice the Z, Y coordinates can also be corrected with respect to S<sub>0</sub> with equations of the same form as equations (5.1), (5.2). A procedure is therefore needed for selecting the most appropriate Correction Factors from equations (4.1) – (4.4) and is illustrated on the Y : Z map of figure 5 (c) . This shows the Y, Z coordinates of a tissue sample (WT) relative to the locus of the reference sectors coordinates (r<sub>0</sub>(T), r<sub>2</sub>(T) with the tissue sample (WT) in the test window. The CF choice is based upon whether WT is nearer to r<sub>0</sub>(T) or r<sub>2</sub>(T) along the Y and Z axes.

For example, figure 5 (b) shows a tissue sample (WT) located relative to the paper calibrating images (W<sub>0</sub>, W<sub>2</sub>) and set values (S<sub>0</sub>, S<sub>2</sub>) (already shown on figure 4). In this case, the tissue corrected (WT)\* was determined with the Correction Factors CF(Z, W<sub>2</sub>), CF(Y, W<sub>2</sub>) since Z(WT) was closer to r<sub>2</sub>(T) than r<sub>0</sub>(T) (figure 5 (c )).

The correction procedure described above is summarised on the **chromatic analysis** flow chart of figure 6.

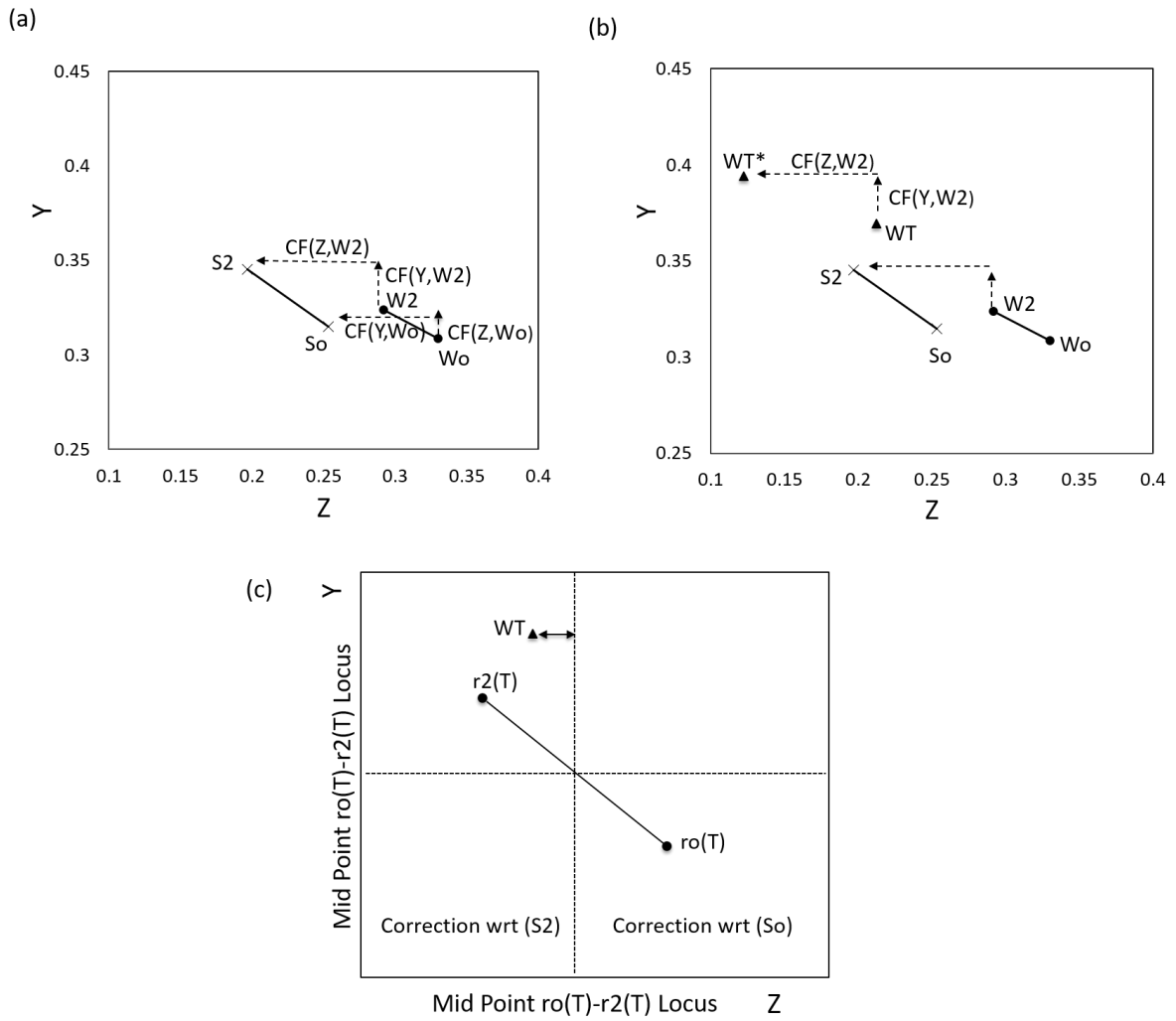


**Figure 5.** Correction of **chromatic Y:Z values obtained from camera images**

(a) Example of a set window locus (Wo-W2) corrected to the set references locus (So-S2) using Samsung (Galaxy SM J10) mobile camera

(b) Example of **deployment** of a Correction Factor (CF(Z, W2)) for a given tissue sample (WT)

(c) Procedure for choosing the most appropriate Correction Factor (CF) for a tissue sample WT with respect to reference areas ro, r2

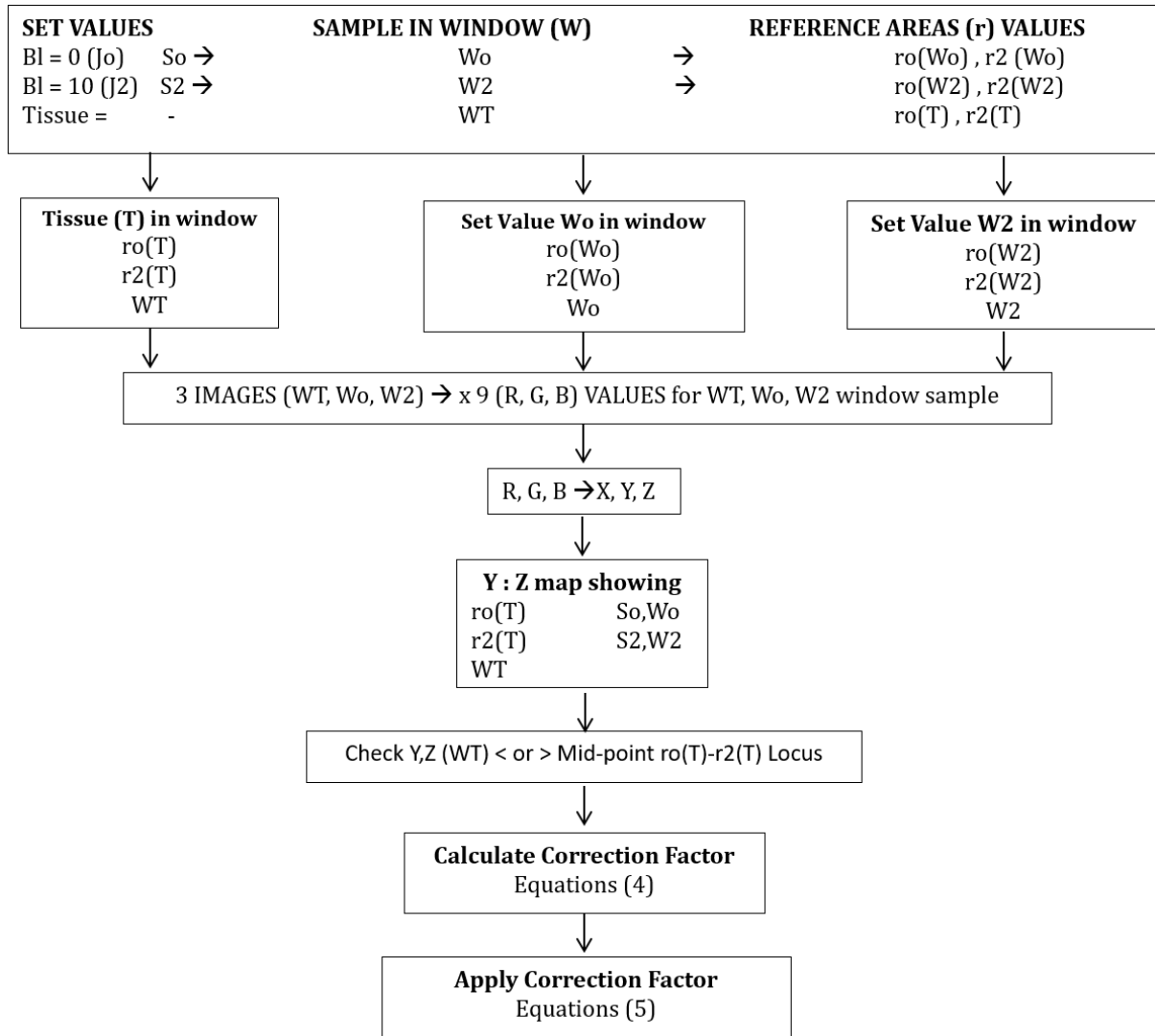


**Figure 6.** Chromatic analysis flow chart

3.2.2. *Secondary Chromatic Calibration Graphs.* Calibration of the corrected **secondary chromatic** parameters  $Y(WT)^*$ ,  $Z(WT)^*$  was achieved with graphs of  $Y(WT)^*$  and  $Z(WT)^*$  versus the corresponding **blood TSB** level. Such calibration graphs have been produced using the 48 neonate samples investigated and are shown on figures 7 (a) for  $Y(WT)^*$  and 7 (b) for  $Z(WT)^*$ . These graphs highlight

- (a) The non-linear variations of both  $Y(WT)^*$  and  $Z(WT)^*$  with **blood** (TSB).
- (b) The opposite trend of  $Y(WT)^*$  and  $Z(WT)^*$  with **blood** (TSB).

The preferred estimate of bilirubin level derived from the chromatic results (SChBl) is taken as the mean of the Y and Z derived values i.e.

$$SChBl = [YCh(Bl) + ZCh(Bl)]/2 \quad (6)$$

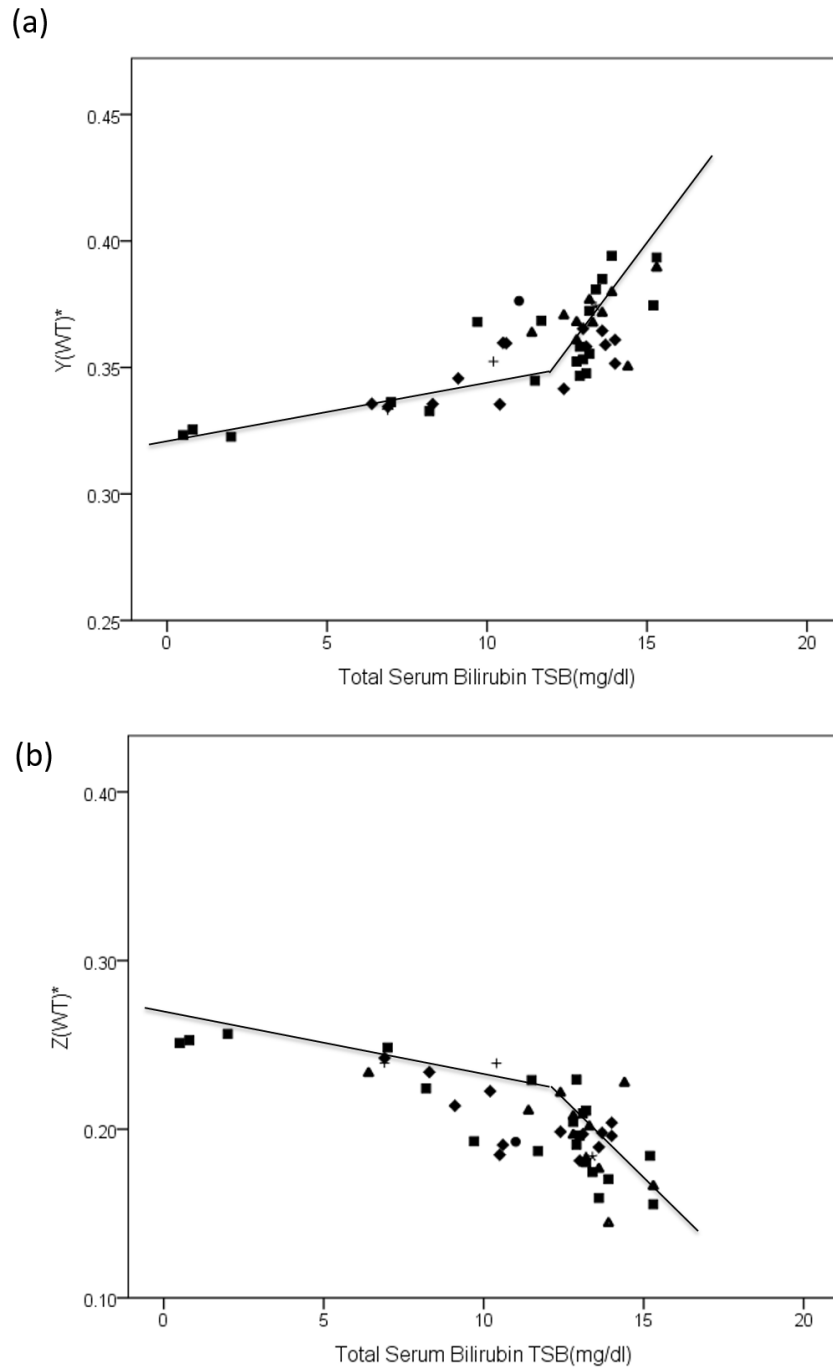


**Figure 7.** Calibration graphs for corrected (WT)\* as a function of Total Serum Bilirubin TSB (mg/dl). (a) Y(WT)\* : TSB, (b) Z(WT)\*: TSB (Mobile phone camera type indicated by symbol of graphical point, Table 1A, Appendix 1)

Figure 8 shows values of the bilirubin levels determined from the test results using the Y(WT)\* and Z(WT)\* calibration graphs of figure 7 (SChBI) as a function of the TSB for the 48 test cases. Also shown on figure 8 as dashed lines are the 95% Prediction Interval boundaries PI(95%) from the fitted regression line (Altman 1991). The scatter of results (e.g. due to melanin etc.) are visible but to a lesser extent than with the Primary Chromatic analysis.

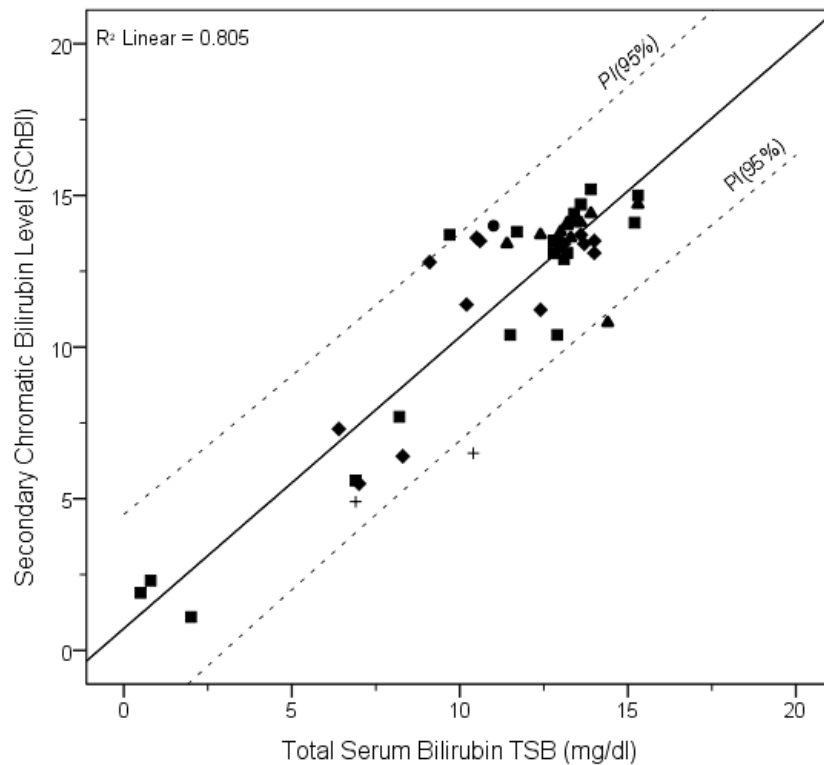


**Figure 8** Corrected **Secondary** Chromatic Bilirubin (SChBI) versus Total Serum Bilirubin (TSB) mg/dl (48 neonates tests, 6 different phone cameras: camera type indicated by symbol of graphical point Table 1A, Appendix 1) Solid line: Regression line, Dashed lines: Prediction Interval boundaries PI(95%)

#### 4. Discussion of Results

The results of the Primary and Secondary Chromatic analysis (figures 3 and 8) may first be compared with **blood test results and optical skin results reported by other researchers then (e.g. Pratesi et al 2015, de Greef et al 2014)**. The comparisons are based upon a Linear Regression analysis (Altman 1991), Bland – Altman plot (Bland et al 1986) and values of Sensitivity (Sn), Specificity (Sp), Positive Predictive Value (PPV), Negative Predictive Value (NPV) (e.g. Deakin et al 2014) (Appendix 2).

##### 4.1 Primary Chromatic Results

A comparison of the Primary Chromatic skin results with the blood test results was first made using a Linear Regression analysis via (SPSS v.21 statistical software) and the results are shown on Table 1. The Primary Chromatic results have a correlation ( $R^2$ ) of 0.43, 95% Confidence Interval CI(95%) (0.43 – 0.88) and a significant level  $P < 0.0001$  and  $F = 34.4$ . Also the experimental Primary Chromatic results of figure 3 show 95% Prediction Interval boundaries PI(95%) of  $\pm 9$  (mg/dl).

Results from a Bland – Altman plot for the Primary Chromatic analysis are also shown on Table 1. These show that the Mean Difference (MD) between the Primary Chromatic analysis and TSB is (-1.24) with 95% Confidence Interval CI(95%) (0 – -2.47) and Limits of Agreement LoA (-7.5 – 5).

**Table 1.** Performance of Primary (PChBI) and Secondary (SchBI) Chromatic Analysis compared with **blood TSB** results for 48 neonates. (Linear Regression: R, R<sup>2</sup>=Correlation Coefficient, CI(95%) = 95% Confidence Interval, F,P=Statistic Significant Values; Bland-Altman Plot: MD= Mean Difference, LoA= MD ±1.96 x standard deviation of difference, CI(95%) = 95% Confidence Interval)

Statistical Analysis Method	Primary Chromatic Analysis (PChBI)	Secondary Chromatic Analysis (SchBI)
Linear Regression	R = 0.65 CI(95%) 0.43 – 0.88 R <sup>2</sup> = 0.43 F = 34.4 P = 4.7*10 <sup>-7</sup>	R = 0.9 CI(95%) 0.77 – 1.03 R <sup>2</sup> = 0.81 F = 190.6 P = 5.7*10 <sup>-18</sup>
Bland – Altman Plot	MD = - 1.24 CI(95%) 0 – -2.47 LoA = -7.5 to 5 CI(95%) ± 2.13	MD = 0.28 CI(95%) 0 – 0.56 LoA = -2.9 to 3.5 CI(95%) ± 0.49

#### 4.2 Secondary Chromatic Results

A comparison of the Secondary Chromatic skin results with blood test results was also made using a Linear Regression analysis via (SPSS v.21 statistical software) and the results are also shown on Table 1. These results have a strong correlation (R<sup>2</sup>) of 0.81, CI(95%) (0.77 – 1.03) and a significant level P < 0.0001 and F = 190. Also the Secondary Chromatic results of figure 8 show PI(95%) of only ±3 (mg/dl).

Results from a Bland – Altman plot (Appendix 3) for the Secondary Chromatic analysis are also shown on Table 1. These show that the MD between the Secondary Chromatic analysis and TSB is (0.28) with CI(95%) (0 – 0.56) and LoA (-2.9 – 3.5). The positive bias along with the CI indicates that the predominant tendency of the Secondary Chromatic approach is to slightly overestimate the bilirubin levels so providing a fail-safe indication of the bilirubin level

#### 4.3. Comparison of the Primary and Secondary Chromatic Analysis Results

A comparison of the Primary and Secondary Chromatic analysis (Table 1) shows that the correlation (R<sup>2</sup>) for the Secondary Chromatic analysis has improved from 0.43 to 0.81, the CI(95%) has improved from (0.43 – 0.88) to (0.77 – 1.03) and the PI(95%) boundaries has improved from ±9 (mg/dl) (figure 3) to ±3 (mg/dl) (figure 8). The correlation and prediction intervals show that the Secondary Chromatic analysis substantially improves the results giving significant correlation with the TSB results.

In addition the Bland - Altman results show that the Secondary Chromatic analysis has a MD of (0.28) compared to (-1.24) for the Primary Chromatic analysis, a CI(95%) of (0 – 0.56) compared with (0 – -2.47) and a LoA (-2.9 to – 3.5) compared to (- 7.5 to 5).

#### 4.4. Comparison of the Secondary Chromatic Results with Other Published Results

A comparison of the Secondary Chromatic results with those obtained with different optical approaches by other researchers may be made in terms of values for the Linear Regression correlation coefficient (R<sup>2</sup>), Sensitivity (Sn), Specificity (Sp), Positive Predictive Value (PPV) and Negative Predictive Value (NPV) (Appendix 2). Values of these parameters have been determined with respect to a critical

**bilirubin** level of 10 mg/dl which corresponds to a typical TSB level of concern for neonates of age after birth up to 48 hours defined by TSB Nomogram (Bhutani 2000). The Secondary Chromatic results are compared with those reported by Pratesi et al (2015) (Bilicare, Minolta JM-103) and de Greef et al (2014) (Bilicam phone) on Table 2.

**Table 2.** Comparison of Secondary Chromatic **analysis** results with other published results. R<sup>2</sup> = Linear Regression Correlation, Sn = Sensitivity, Sp = Specificity, PPV = Positive Predictive Value, NPV= Negative Predictive value for a **critical bilirubin level** 10 mg/dl.

Source	No. Tests	R <sup>2</sup>	Sn	Sp	PPV	NPV
1. (Pratesi et al 2015)						
(a) Bilicare	97	0.31	0.96	0.4	0.86	0.73
(b) Minolta JM-103	98	0.49	0.81	0.74	0.83	0.73
2. (de Greef et al 2014)						
Bilicam (phone)	100	0.71	0.82	0.8	0.81	0.81
3. Secondary Chromatics Analysis SCh(B)l	48	0.81	0.97	0.82	0.95	0.90

The Secondary Chromatic results have high values of Sensitivity (0.97), Specificity (0.82), PPV (0.95) and NPV (0.90) indicating a high capability for identifying critical cases. These values are higher than the values quoted by Pratesi et al (2015) (Bilicare, Minolta JM-103) and de Greef et al (2014) (Bilicam (phone)). Also the **correlation coefficient** (R<sup>2</sup>) of the Secondary Chromatic results (0.81) is higher than those of the Pretesi and de Greef value (0.31 – 0.71).

Taylor et al (2017) have more recently quoted good results for a Bilicam system but based upon a higher critical Bilirubin level of 17 mg / dl rather than the 10 mg / dl critical level **for** the present results.

#### 4.5. Results with Different Mobile Phone Cameras

The results presented were obtained with 6 different types of mobile phone cameras (Appendix 1). These show that the non-linear Secondary Chromatic analysis accommodates the use of these different cameras to provide bilirubin level results which are largely independent of the type of camera used. Checks made with a further 6 different cameras using only reference images (Appendix 1) indicate that the camera responses are similar to the 6 cameras used in the skin tests. Thus reliable skin tissue results should be produced from a larger range of different cameras than the limited number of cameras used in the present tests.

#### 4.6. Effects of Other Skin Tissue Component

Skin tissue components, other than **bilirubin**, can affect the values of the chromatic parameters X, Y, Z, L. In the present tests, the effect of haemoglobin (figure 2) was reduced by occluding the skin tissue. The effect of melanin is partly taken into account via the set calibrations (So, S2) because the values of these parameters were derived from images of real neonate skin tissue which contained melanin and not based upon pure **bilirubin** spectra. The correction procedure with the Secondary Chromatic analysis (Figures 5) appears to reduce the effect of any melanin variations between different neonates. This is apparent as a reduced scatter of the results which lie within **PI(95%)** boundaries  $\pm 3\text{mg/dl}$  (figure 8). Larger variations in melanin levels due for instance to different ethnic skins will require further study. **The effect of biliverdine occurrence in the skin should also be investigated further. The chromatic**



approach has sufficient flexibility for accommodating such effects as further empirical information emerges by, for example adjustments to the chromatic calibrations, more detailed attention to longer wavelengths via the R parameter etc.

## **5. Conclusions**

It has been shown that the skin jaundice of a neonate can be monitored using a new chromatic analysis of data obtained with a mobile phone and a novel template (Shabeer et al 2016).

A non-linear form of the chromatic analysis produces skin tissue results (TcB) which are in good agreement with blood analysis (TSB) results having a high correlation ( $R^2$ ) of 0.81 and a mean difference (MD) of 0.28 mg/dl. The results indicated that neonates with bilirubin levels above a medically regarded critical level 10 mg/dl early after birth could be identified with a high degree of Sensitivity (0.97), Specificity (0.82), PPV (0.95) and NPV (0.9) higher than those reported to date with other optical systems Pratesi et al (2015) (Bilicare, Minolta JM-103) and de Greef et al (2014) (Bilicam).

The method has been shown to be useable with at least 6 different types of mobile phones.

Bilirubin levels can be distinguished to within  $\pm 3$  mg/dl which is sufficient to provide an indication as to whether a more detailed bilirubin blood test should be sought.

Further investigations should include the use of a greater variety of mobile phones than the 6 phones already tested, addressing a wider variety of ethnic skins, applications to skin conditions following phototherapy etc.

## **Acknowledgements**

The inputs by various colleagues in contributing to this study are appreciated – Dr. D. Smith for tuning the template design; Mr Viju & Ms. F. Zahra in contributing to the design of the template holder; Dr. R. Ferrero, Dr. A. Al-Temeemy, Dr. Z. Almajali in contributing to the software development; Dr. P. Venkattagiri for clinical inputs.

## APPENDIX 1

### Camera used in the study along with their pixel densities

Table 1A. Mobile phone cameras and their resolutions used in the chromatic tests on 48 neonates

Phone Camera Model	Resolution (Mega-Pixels)	Symbol	Number of tests
Apple (iPhone 4)	0.8	●	1
Samsung (GT-S6802)	1.2	▲	10
Samsung (SM-J200G)	3	+	2
Micromax (A-106)	5	*	1
Xiomi (Redmi 2014818)	8	■	20
Oneplus (ONE-E1003)	8.3	◆	14

Table 1B. Additional Mobile phone cameras and their resolutions used only for addressing references (Wo, W2) for supplementary information

Phone Camera Model	Resolution (Mega-Pixels)	Symbol
Samsung (Galaxy SMJ 10)	3	○
LG (P875)	1	×
Samsung SM-J2L10F)	8	◇
Samsung (SM-J200G)	5	–
Lenova (A2010a)	0.7	□
Micromax (A106)	0.7	△

## APPENDIX 2

### Formula for Sensitivity, Specificity, PPV, NPV

Sensitivity (**Sn**), Specificity (**Sp**), Positive Predicted Value (PPV), Negative Predicted Value (NPV) are defined by the following equations (e.g. Deakin et al (2014))

$$\text{Sensitivity (Sn)} = TP(ChI) / (TP(ChI) + FN(ChI)) \quad (A.1)$$

$$\text{Specificity (Sp)} = TN(ChI) / (TN(ChI) + FP(ChI)) \quad A.2$$

$$\text{Positive Predicted Value (PPV)} = TP(ChI) / (TP(ChI) + FP(ChI)) \quad (A.3)$$

$$\text{Negative Predicted Value (NPV)} = TN(ChI) / (TN(ChI) + FN(ChI)) \quad (A.4)$$

Where TP(ChI), FP(ChI) are respectively the number of True, False **positive chromatic results** (Bl > or = 10).

TN(ChI), FN(ChI) are respectively the number of True, False **negative chromatic results** (Bl <10)

(ChI – Chromatic Indicator)

### APPENDIX 3

#### Bland-Altman Plot (Secondary Chromatic analysis)

A Bland – Altman plot for the Secondary Chromatic analysis is shown on figure A3.1. This figure shows a graph of the difference between the bilirubin results of the Secondary Chromatic analysis (SChBI) and the TSB results (i.e. (SChBI minus TSB) plotted against their average

The MD between the chromatic and TSB results is represented on figure A3.1 as the separation of the two horizontal solid lines which has a value of (0.28) and with a CI(95%) of (0 – 0.56).

Figure A3.1 also shows the LoA between the Secondary Chromatic and TSB results as two dashed horizontal lines (based upon  $MD \pm 1.96$  standard deviation of the difference). This shows that the 95% difference lies between the limits (-2.9) – (3.5) mg/dl. Thus 95% of neonates tested with the Secondary Chromatic approach would be indicated to have between 2.9 units less and 3.5 units greater than the blood TSB measurement.

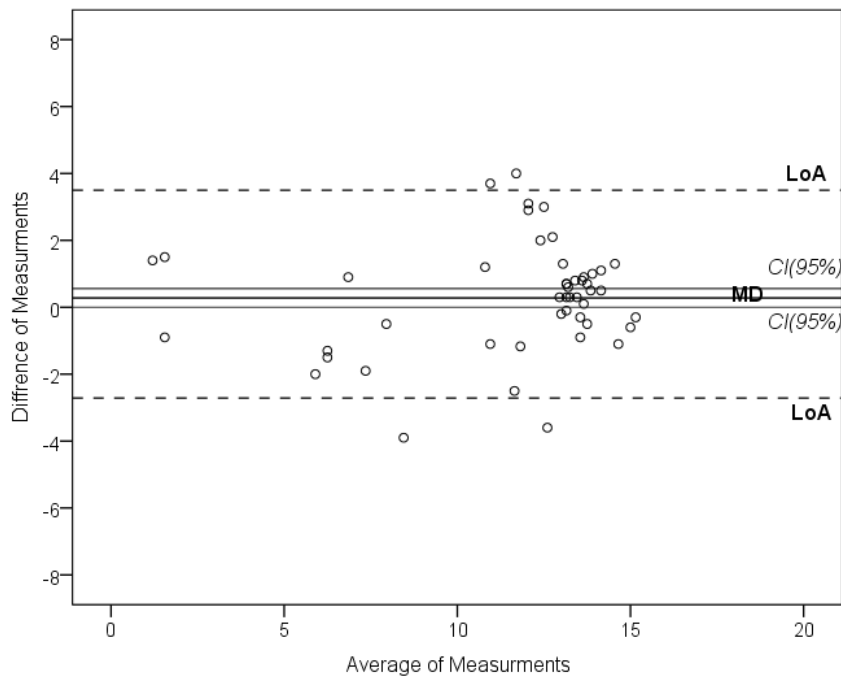


**Figure A3.1.** Bland-Altman plot showing the difference between Secondary Chromatic bilirubin (SchBI) and TSB blood measurements against their average. Difference of measurements = [SchBI Minus TSB]; Average of measurements =  $[(SchBI + TSB) / 2]$ ; Solid black lines: MD and (CI 95%); Dashed lines: Limit of Agreement (LoA)

## References

- Altman D G (1991) *Practical Statistics for Medical Research* (London, Chapman & Hall) ISBN: 0412276305
- Bertini G, Pratesi S, Cosenza E, Dani C. (2008) Transcutaneous bilirubin measurement: evaluation of Bili test, *Neonatology* **93**,101-105
- Biliscan, n.d., A Portable non-invasive transcutaneous bilirubin analysis instrument, Löwenstein Medical. Available from: <https://hul.de/en/produkt/biliscan/?ref=en.hul.de> [13 October 2017]
- Bhutani V K, Gorley G R, et al (2000) Noninvasive measurement of total Bilirubin in a multiracial predischarge newborn population to assess the risk of severe hyperbilirubinemia, *Pediatrics* **106** (2), e17)
- Bland J M, Altman D (1986) Statistical methods for assessing agreement between two methods of clinical measurements, *Lancet* 327 307 310
- Bosschaart N, Mentink R, Kok j H, van Leeuwen T G, Aalders M C G. (2011) Optical properties of neonatal skin measured in vivo as a function of age and skin pigmentation, *J. of Biomedical Optics* **16** (9), 097003
- Bosschaart N, Kok H K, Newsum A M, Ouweneel D M, Mentink R, van Leeuwen T G, Aalders C G (2012) “Limitations and Opportunities of Transcutaneous Bilirubin Measurements”, *Pediatrics* **129**
- Dai J, Parry D M, Krahn J, (1997) Transcutaneous bilirubinometry: its role in the assessment of neonatal jaundice, *Clinical Biochemistry* **30** (19)
- Deakin A G, Jones G R, Spencer J W, Bongard E J, Gal M, Sufian A T, Butler C C. (2014) “A portable system for identifying urinary tract infection in primary care using a PC-based chromatic technique”, *Physiol. Meas.* **35** 793-805
- De Greef L, Goel M, Seo M J, Larson E C, Stout J W, Taylor J A, Patel S N. (2014). “Bilicam: using mobile phones to monitor newborn jaundice’, In *Proceedings of the ACM International Joint Conference on Pervasive and Ubiquitous Computing*. ACM, New York, NY, USA, 331-342. DOI: <https://doi.org/10.1145/2632048.2632076>
- De Luca D, Zecca E, Corsello M, Tiberi E, Semeraro C, Romagnoli C. (2008) Attempt to improve transcutaneous bilirubinometry: a double blinded study Medick BiliMed versus Respiroics BiliCheck, *Archives of Disease in Childhood–Fetal and Neonatal edition* **93**,135-139
- Dennery, P A, Seidman D S, Stevenson D K (2001) Neonatal Hyperbilirubinemia. *The New England Journal of Medicine* **344** 581-589
- Elzagzoug E, Jones G R, Deakin A G, Spencer J W (2014) Condition monitoring of high voltage transformer oils using optical chromaticity *Meas. Sci. Technol.* **25** 065205
- Jones G R, Deakin A G, Brookes R J, and Spencer J W (2009a) A portable liquor monitoring system using a PC-based chromatic technique, *Meas. Sci. Technol.* **20** 075305
- Jones G R, Deakin A G, and Spencer J W (ed), 2008 *Chromatic Monitoring of Complex Conditions* (Boca Raton, FL: CRC Press) ISBN: 9781584889885

KJ-8000, n.d., A portable instrument that measures transcutaneous bilirubin value relating to serum bilirubin value of new-borns and infants, Kejian Hi-tech. Available from: <http://www.kejianmed.com/bilirubin-meter-Jaundice-meter.htm> [13 October 2017]

Lilien I D, Harris V J, Ramamurthy R S, Pildes R S, (1976) Neonatal osteomyelitis of the calcaneus: complication of heel puncture, *The Journal of Pediatrics* **88** 478-480

Lo C K, Loo H, M, Sufian, A T, Jones G R, Spencer J W. (2017). Transformer Oil Degradation Monitoring Analyzed by Optical Fluorescence. *Proceeding of the International Conference on Imaging, Signal Processing and Communication (ICISPC)*, Penang, Malaysia. ACM, New York, NY, USA

Maisels M J, Kring E, (1997) Transcutaneous bilirubinometry decreases the need for serum bilirubin measurements and saves money, *Pediatrics* **99**,599601

Maisels M J, Baltz R D, Bhutani V K, Newman T B, Palmer H, Rosenfeld W, Stevenson D K, Weinblatt H B, (2004) Clinical Practice Guideline: management of hyperbilirubinemia in the newborn infant 35 weeks of gestation, *Pediatrics* **114** 297-316.

Namba F, Kitajima H, 2007 Utility of a new transcutaneous jaundice device with two optical paths in premature infants *Pediatrics International* **49** 497-501

Petersen J R, Okorodudu A O, Mohammad A A, Fernando A, Shattuck K E. (2005) Association of transcutaneous bilirubin testing in hospital with decreased readmission rate for hyperbilirubinemia, *Clinical Chemistry* **51** 510-544

Polley N, Saha S, Singh S, Adhikari A, Das S, Choudhury B R, Pal S K (2015) Development and optimization of a noncontact optical device for online monitoring of jaundice in human subjects, *Journal of Biomedical Optics* 20 (6) 067001

Polley N, Saha S, Adhikari A, Banerjee S, Darbar S, Das S, Pal S K (2015) Safe and symptomatic medical use of surface-functionalized Mn<sub>3</sub>O<sub>4</sub> nanoparticles for hyperbilirubinemia treatment in mice. *Nanomedicine (Lond.)* (2015) 10(15), 2349–2363

Petersen J R, Okorodudu A O, Mohammad A A, Fernando A, Shattuck K E. (2005) Association of transcutaneous bilirubin testing in hospital with decreased readmission rate for hyperbilirubinemia, *Clinical Chemistry* **51** 510-544

Pratesi S, Boni L, Tofani L, Berti E, Sollai S, Dani C (2015) Comparison of the transcutaneous bilirubinometers Bilicare and Minolta JM-103 in late preterm and term neonates, *J. of maternal-fetal and Neonatal Medicine* Taylor and Francis. DOI: 10.3109/ 14767058.2015.1113521

Puppalwar P V, Goswani K, Dhok A. (2012) Review on evolution of methods of Bilirubin Estimation. International Organisation of Scientific Research, *Journal of Dental & Medical Science (ISOR-JDMS)* **1**(3) 17-28

Rubaltelli F F, Gourley G R, Loskamp N, Modi N, Kleiner M R, Sender A, Vert P. (2001) Transcutaneous bilirubin measurement: a multi center evaluation of a new device, *Pediatrics* **107**, 1264-1271

Sarkar P K, Pal S, Polly N, Aich R, Adhikari A, Halder A, Chakrabarti S, Chakrabarti P, Pal S K (2017) Development and validation of a noncontact spectroscopic device for haemoglobin estimation at point-of care, *Journal of Biomedical Optics* 22 (5) 055006

Shabeer H M, Jones G R, Spencer J W, Sufian A T, Elzagzoug E Y, Smith D H, Viju T S, Zhra F, 2016 Chromatic Mobile Phone Accessory, Government of India Patent Office, Certificate of Design Registration No. 288654.

Tayaba R, Gribetz D, Gribetz I, Holzmann I R. (1998) Noninvasive estimation of serum bilirubin, *Pediatrics* **102**(28)

Taylor J A, Stout W, degree L, Goel M, Patel S. Chung E. S, Koduri A, McMahon S, Dickerson J, Simpson E A, Larson E C (2017) Use of a Smartphone App to assess Neontatal Jaundice, *Pediatrics* **140**(3)

Watson D. (1961) Analytic methods for bilirubin in blood plasma, *Clinical Chemistry*, **7**, 603-625

Yamanouchi, Y. Yamauchi, I. Igarashi. (1980) Transcutaneous Bilirubinometry: Preliminary Studies of Non invasive Transcutaneous Bilirubin Meter in the Okayama National Hospital, *Pediatrics* **65** 195- 202

Yasuda S, Itoh S, Isobe K, Yonetani M, Nakamura H , Nakamura M, Yamauchi Y, Yamanishi A. (2013) New transcutaneous jaundice device with two optical paths, *Journal of Perinatal Medicine* **31** 81-88

## **List of Figures**

### **Figure 1. Optical measurement system and image produced**

(a) Schematic diagram of the system layout

(b) Typical images captured by a mobile phone camera of  $W_0$  (set Bl = 0),  $W_2$  (set Bl = 10mg/dl) and WT (neonate nose tissue) in the sample window and set references  $r_0$  = (set Bl  $\approx$  0),  $r_2$  = (set Bl  $\approx$  10)

**Figure 2.** Typical overlapping wavelength responses (R, G, B) of an electronic camera relative to wavelength ranges of some skin tissue components (Bilirubin (Bl), Haemoglobin (He), Melanin (Me))

**Figure 3.** Primary Chromatic Bilirubin level (PChBl) versus Total Serum Bilirubin (TSB) mg/dl. (Results for 48 neonate tests with 6 different phone cameras; each camera type designated by symbols from Table 1A). Solid line: Regression line, Dashed lines: Prediction Interval boundaries PI(95%)

**Figure 4.** Chromatic Y : Z map showing set reference areas locus ( $S_0$ - $S_2$ ) and set sample window loci ( $W_0$ - $W_2$ ) for 12 different cameras with set reference ( $S_0$ - $S_2$ ), 6 mobile phone cameras used in the neonate tests (Table 1A, Appendix 1) full lines, 6 mobile phone cameras used in reference tests only (Table 1B, Appendix 1) dashed lines.

### **Figure 5. Correction of chromatic Y:Z values obtained from camera images**

(a) Example of a set window locus ( $W_0$ - $W_2$ ) corrected to the set references locus ( $S_0$ - $S_2$ ) using Samsung (Galaxy SM J10) mobile camera.

(b) Example of deployment of a Correction Factor (CF(Z,  $W_2$ )) for a given tissue sample (WT)

(c) Procedure for choosing the most appropriate Correction Factor (CF) for a tissue sample WT with respect to reference areas  $r_0$ ,  $r_2$

### **Figure 6. Chromatic analysis flow chart**

**Figure 7.** Calibration graphs for corrected (WT)\* as a function of Total Serum Bilirubin (TSB) mg/dl. (a) Y(WT)\* : TSB, (b) Z(WT)\*: TSB (Mobile phone camera type indicated by symbol of graphical point, Table 1A, Appendix 1)

**Figure 8** Corrected Secondary Chromatic Bilirubin (SchBl) versus Total Serum Bilirubin (TSB) mg/dl (48 neonates tests, 6 different phone cameras: camera type indicated by symbol of graphical point Table 1A, Appendix 1) Solid line: Regression line, Dashed lines: Prediction Interval boundaries PI(95%).

## List of Tables

**Table 1.** Performance of Primary (PChBl) and Secondary (SchBl) Chromatic Analysis compared with blood TSB results for 48 neonates. (Linear Regression: R, R<sup>2</sup>=Correlation Coefficient, CI(95%) = 95% Confidence Interval, F,P=Statistical significant values; Bland-Altman Plot: MD= Mean Difference, LoA= MD ±1.96 x standard deviation of difference, CI(95%) = 95% Confidence Interval)

**Table 2.** Comparison of Secondary Chromatic Analysis results with other published results. R<sup>2</sup> = Linear Regression correlation, Sn = Sensitivity, Sp = Specificity, PPV = Positive Predictive Value, NPV= Negative Predictive value for a critical bilirubin level 10 mg/dl.

## APPENDICES

APPENDIX 1: Camera used in the study along with their pixel densities

Table 1A. Different Mobile phone cameras and their resolutions used in the chromatic tests on 48 neonates

Table 1B. Additional Mobile phone cameras and their resolutions used only for addressing references (Wo, W2) for supplementary information

APPENDIX 2: Formula for Sensitivity, Specificity, PPV, NPV

APPENDIX 3 : Bland-Altman Plot (Secondary Chromatic analysis)

**Figure A3.1.** Bland-Altman plot showing the difference between Secondary Chromatic bilirubin (SchBl) and TSB blood measurements against their average. Difference of measurements = [SchBl Minus TSB]; Average of measurements = [(SchBl + TSB) / 2]; Solid black lines: MD and (CI 95%); Dashed lines: Limit of Agreement (LoA)